Amplification of the North American "Dust Bowl" drought through human-induced land degradation

Benjamin I. Cook[a,b,1], Ron L. Miller[b], and Richard Seager[a]

[a]Lamont–Doherty Earth Observatory, 61 Route 9W, Palisades, NY 10964; and [b]NASA Goddard Institute for Space Studies, 2880 Broadway, New York, NY, 10024

Edited by James E. Hansen, Goddard Institute for Space Studies, New York, NY, and approved February 3, 2009 (received for review October 13, 2008)

The "Dust Bowl" drought of the 1930s was highly unusual for North America, deviating from the typical pattern forced by "La Nina" with the maximum drying in the central and northern Plains, warm temperature anomalies across almost the entire continent, and widespread dust storms. General circulation models (GCMs), forced by sea surface temperatures (SSTs) from the 1930s, produce a drought, but one that is centered in southwestern North America and without the warming centered in the middle of the continent. Here, we show that the inclusion of forcing from human land degradation during the period, in addition to the anomalous SSTs, is necessary to reproduce the anomalous features of the Dust Bowl drought. The degradation over the Great Plains is represented in the GCM as a reduction in vegetation cover and the addition of a soil dust aerosol source, both consequences of crop failure. As a result of land surface feedbacks, the simulation of the drought is much improved when the new dust aerosol and vegetation boundary conditions are included. Vegetation reductions explain the high temperature anomaly over the northern U.S., and the dust aerosols intensify the drought and move it northward of the purely ocean-forced drought pattern. When both factors are included in the model simulations, the precipitation and temperature anomalies are of similar magnitude and in a similar location compared with the observations. Human-induced land degradation is likely to have not only contributed to the dust storms of the 1930s but also amplified the drought, and these together turned a modest SST-forced drought into one of the worst environmental disasters the U.S. has experienced.

dust aerosols | land surface feedbacks

Recurrent periods of drought are a common feature of the mid-latitudes, including North America, modulated on interannual and decadal time scales primarily by the El Nino Southern Oscillation (1–6). Over North America, drier than normal conditions occur in the southwest and southeast United States when SSTs in the eastern tropical Pacific are lower than normal ("La Nina" conditions). Drought over North America is also tightly linked to warm SSTs in the North Atlantic, especially on decadal time scales (7, 8). Typical examples of recent La Nina droughts in North America include the drought of the 1950s (3) and the most recent drought at the beginning of the 21st century (8, 9), events that have been successfully modeled in GCMs when forced by observed SSTs (3, 7–9). La Nina conditions, with additional forcing from warm Atlantic SSTs, have also been implicated as the initial causes of the 1930s drought known as the "Dust Bowl" (1, 2, 4), with some speculation that soil moisture feedbacks may have amplified the drought (1). The Dust Bowl was a significant disaster for the United States, resulting in large economic and agricultural losses, farm abandonment, and a level of human migration that, in the recent historical period, is comparable only with the evacuation of New Orleans in 2005 (4, 10). However, the Dust Bowl differed in important ways from the canonical La Nina drought pattern (Figs. 1 *Left*) (11). These differences include the anomalous warmth and the intensity of the drought, given the modest size of the La Nina SST anomaly observed during the 1930s, and the movement of the drought center from the southwest and Mexico into the Central Great Plains. Models forced with observed SSTs during the 1930s produce a drought (1, 2, 4) that is centered too far south and fail to replicate the near continental-scale warm anomaly centered in the northern United States (Fig. 1 *Center*). This implies either some deficiencies in the models or, alternatively, some missing physical processes.

One hypothesis regarding the atypical Dust Bowl drought pattern invokes large-scale changes to the land surface during this time period. During the 1920s, agriculture in the United States expanded into the central Great Plains. Much of the original, drought-resistant prairie grass was replaced with drought-sensitive wheat. With no drought plan and few erosion-control measures in place, this led to large-scale crop failures at the initiation of the drought, leaving fields devegetated and barren, exposing easily eroded soil to the winds. This was the source of the major dust storms and atmospheric dust loading of the period on a level unprecedented in the historical record (e.g., refs. 12–15). We hypothesize that the dust storms and the loss of vegetation amplified the La Nina forced drought and caused the anomalous pattern of temperature and precipitation. Changes in climate and weather have been linked to vegetation changes and soil dust aerosols for other regions of the world (16–18), and the importance of land surface feedbacks during the Dust Bowl has been suggested previously (1, 5, 19). Few studies, however, have quantitatively tested the joint impact of dust aerosols and vegetation loss during this period.

We use the Goddard Institute for Space Studies atmospheric GCM (GISS ModelE, details below) to test our hypothesis that land degradation during the period can explain the anomalous features of the drought. GISS ModelE, when forced with observed SSTs, reproduces other examples of SST-related hydroclimatic variability, such as the North American drought of the 1950s [Supporting Information (SI)]. We conducted 4 suites of 5-member ensemble simulations using observed SSTs from 1932 to 1939, with each ensemble member starting from different initial conditions. In SST-ONLY, observed global SSTs (1932–1939) force the model, with no modifications to the land surface. In SST+DUST, we added a dust aerosol source over the Plains, over the approximate region of wind erosion during the period (Fig. 2 *Left*). Ensemble average net dust emission (emission minus deposition) from our Great Plains dust source in this simulation was 369 million metric tons per year, a magnitude consistent with the limited available estimates of soil loss (SI). The spatial pattern of the ensemble average dust aerosol loading (Fig. 2 *Middle*) is quite similar to qualitative dust storm maps of the period (12, 13), although no quantitative information is

Author contributions: B.I.C. designed research; B.I.C. performed research; R.L.M. and R.S. contributed new reagents/analytic tools; B.I.C., R.L.M., and R.S. analyzed data; and B.I.C. wrote the paper.

The authors declare no conflict of interest.

This article is a PNAS Direct Submission.

[1]To whom correspondence should be addressed. E-mail: bc9z@ldeo.columbia.edu.

This article contains supporting information online at www.pnas.org/cgi/content/full/0810200106/DCSupplemental.

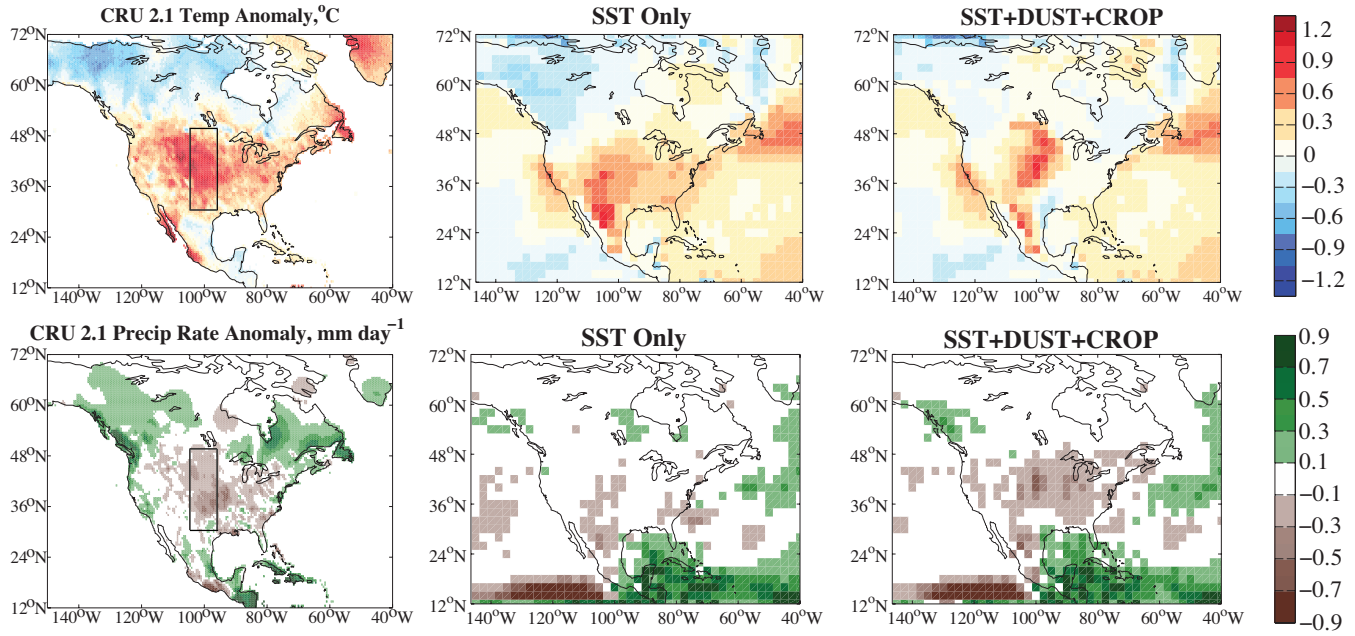

Fig. 1. Temperature (°C) and precipitation (mm day^{-1}) anomalies for the Dust Bowl drought from the Climate Research Unit (CRU) version 2.1 dataset (11) and 2 of our model experiments: SST-ONLY (our control) and SST+DUST+CROP (full land degradation in the form of a Great Plains dust aerosol source and crop removal). The CRU data are composed of monthly climate grids for the world, statistically interpolated from station observations to continuous 0.5° spatial resolution. Model grid spacing is ≈2° × 2.5°. Anomalies are for the period 1932–1939, relative to the 1920–1929 observed average (for CRU data) or an ensemble average from a 5-member ensemble run using observed SSTs for 1920–1929 (for the model plots). The block rectangle in the CRU plot surrounds the Great Plains region (105°E–95°E and 30°N–50°N), used to calculate spatially averaged anomalies for Fig. 3.

currently available. In SST+CROP, we simulated vegetation losses associated with the crop failure by converting the crop areas over the Great Plains to bare soil (Fig. 2 *Right*), leading to fractional vegetation reductions of almost 50% in some grid cells. Finally, in our SST+DUST+CROP experiment, the model was forced with observed SSTs, along with a full representation of crop failure via inclusion of both a dust source over the Plains and vegetation reductions.

All model-based anomalies are calculated relative to an ensemble forced by using observed SSTs from 1920 to 1929 to enable comparison with the observed anomalies from the CRU 2.1 dataset (11). The model ensemble forced with SSTs alone produces only a modest drying and warming over the Great Plains region (Fig. 1 *Center*). When both land surface forcings are included (SST+DUST+CROP), the temperature and precipitation anomalies are amplified to the observed level, and the drought is now correctly centered over the central and northern Great Plains (Fig. 1 *Right*). Fig. 3 displays the annual temperature and precipitation anomalies for each ensemble, averaged over the Great Plains region (105°E–95°E and 30°N–50°N, highlighted by the black rectangle in Fig. 1). Vegetation feedbacks (SST+CROP) shift the temperature distribution toward warmer values, and this is the only ensemble whose members reach the extreme values seen in the CRU data. The warm anomaly is reduced when dust aerosols are added, but a region of strong warming from crop devegetation remains in the northern Plains. The addition of a dust source (SST+DUST and SST+DUST+CROP), however, has a large impact on precipitation, drying out much of the Great Plains and shifting the precipitation anomaly distribution over the Great Plains to more negative values.

The feedbacks (vegetation and dust) and their impacts can be best understood by isolating each factor in separate ensemble experiments (Fig. 4). Area-averaged top of the atmosphere (TOA) radiation balance and surface fluxes for each of our simulations are shown in Table 1. Different mechanisms explain the temperature and precipitation anomalies. Removal of vegetation (SST+CROP) reduces total evapotranspiration from the

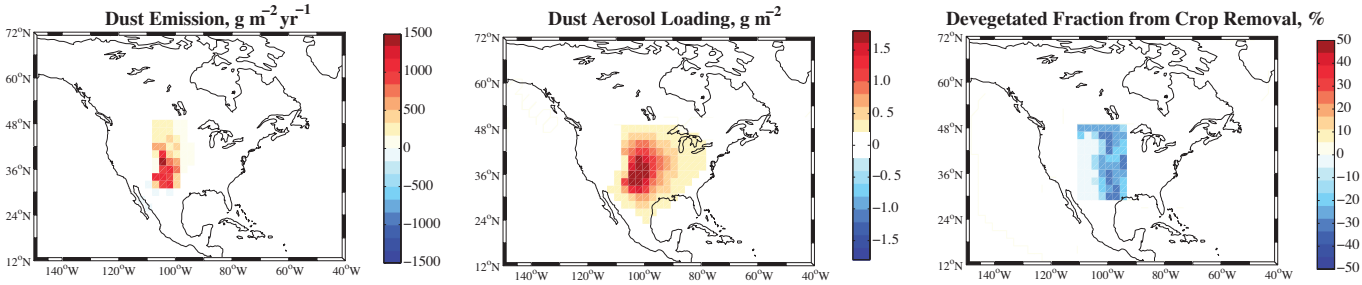

Fig. 2. Dust emission (*Top*, g m^{-2} y^{-1}) and dust aerosol loading (*Middle*, g m^{-2}) from the SST+DUST experiment and devegetated fraction (*Bottom*, %) from the SST+CROP experiment, relative to SST-ONLY for 1932–1939. The devegetated fraction is identical in the SST+DUST+CROP experiment, and the dust emissions and loading are similar (discussed further in the SI).

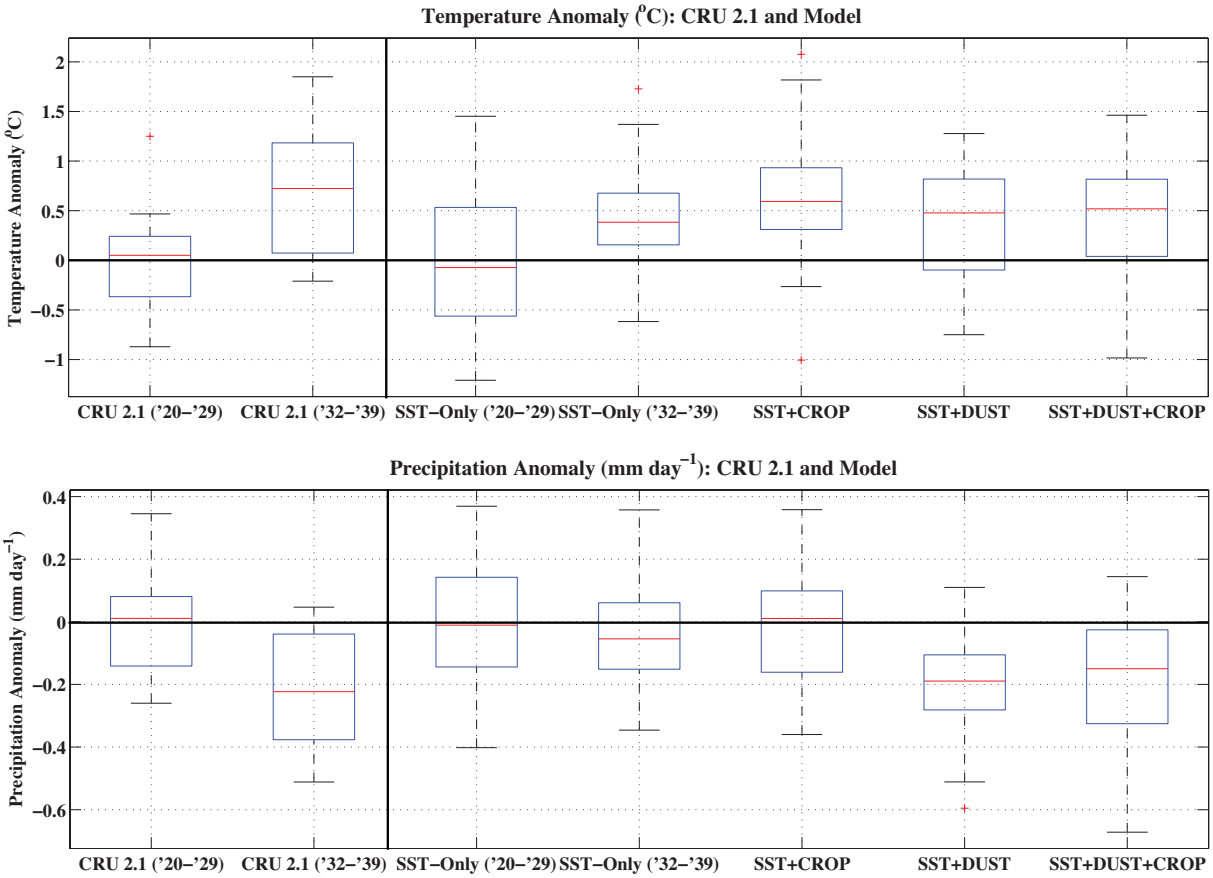

Fig. 3. Box-and-whisker plots for precipitation and temperature anomalies from the CRU 2.1 data and each ensemble member (SST-Only, SST+CROP, SST+DUST, SST+DUST+CROP). Anomalies (in mm/day) are averaged over the Great Plains region (105°E–95°E and 30°N–50°N), the same area as in Fig. 1. Anomalies are for the period 1932–1939, relative to the 1920–1929 observed average (for CRU data) or an ensemble average from a 5-member ensemble run using observed SSTs for 1920–1929 (for the model plots). The boxes indicate the lower quartile, median, and upper quartile values, and the whiskers mark the most extreme values within 1.5 times the interquartile range. Outliers, values falling beyond the whiskers, are marked with the red crosses.

land surface by severely limiting transpiration, the flux of water from the soil to the atmosphere through plants during photosynthesis. Over the main region of impact at the surface (100°W–90°W, 35°N–50°N), decreased summertime evapotranspiration, mostly compensated by increased sensible heating, raises the Bowen ratio from 0.52 (SST-ONLY) to 0.59 (SST+CROP). This leads to increased soil and near-surface air temperatures. Warming during the summer is carried over into the fall and winter seasons by positive soil temperature anomalies, when these warmer soils release this heat to the atmosphere (SI).

The addition of a dust source, and subsequent increase in dust aerosol loading (SST+DUST), reduces net radiation at TOA and at the surface largely by shortwave reflection (Table 1 and SI). To balance, a compensatory increase in atmospheric energy input is required, manifesting as upper-level convergence and low-level divergence, reflected in geopotential height anomalies at 850 hPa, 500 hPa, and 300 hPa (SI). This indicates anomalous subsidence, inhibiting convection and cloud development, and reducing moisture convergence into the region (SI), leading to a subsequent reduction in precipitation and a shift of the drought center northward over the central Great Plains, near the center of the dust aerosol cloud. Note that the precipitation anomaly is slightly positive in the SST+CROP experiment, consistent with the net radiative anomaly at TOA.

When the effects of dust and crop removal are combined (SST+DUST+CROP), feedbacks from the separate experiments act in concert to augment the impact of SST forcing, simultaneously warming the surface and reducing precipitation. The reduction in transpiration by the removal of crops in the combined experiment causes warming that is only slightly reduced compared with the effect of crops alone, because the reduction in net TOA radiation by dust causes only a slight offset to surface temperature. Similarly, precipitation is reduced in the combined experiment as in the dust-only case, because the TOA radiative anomaly is dominated by the effect of dust. Our improved simulation of temperature and precipitation anomalies, when more realistic land surface boundary conditions are included, suggests that land surface feedbacks from the human-induced land degradation are a necessary ingredient to explain the atypical nature of the Dust Bowl drought.

As with many simulations of historical climate, we are limited by observational uncertainties during the period. Climate records over North America are fairly reliable (11), but few quantitative estimates of dust emission, aerosol loading, or even magnitude of crop failure are available. Spatial extent of the Great Plains dust source area and crop removal are based on a map of soil erosion, from ref. 10. These issues are discussed further in the SI. The forcing from the dust aerosols tends to ameliorate the warming associated with crop failure, as seen in experiments SST+DUST+CROP. Shortwave reflection may be overestimated in our model, and cooling associated with the dust aerosols may be too high. Still, the precipitation pattern is well resolved in both SST+DUST and SST+DUST+CROP, and the temperature anomaly suggests that the crop failure contributed to the anomalous warmth during the period.

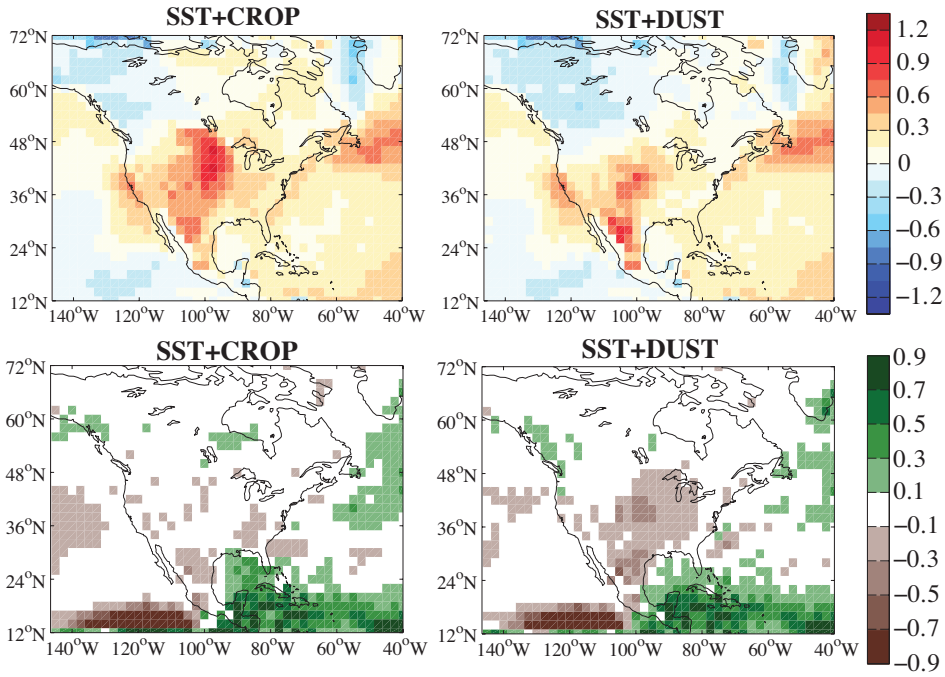

Fig. 4. Spatial pattern for temperature (°C) and precipitation (mm day^{-1}) anomalies for the Dust Bowl drought from our individual surface feedback experiments: SST+CROP (crop removal) and SST+DUST (Great Plains dust aerosol source). Anomalies are relative to an ensemble average from a 5-member ensemble run using observed SSTs for 1920–1929.

The results from this study suggest a mechanism that could explain some of the anomalous drought patterns during the last thousand years, as seen in proxy reconstructions from tree ring records (20, 21). The Dust Bowl drought was likely unique during the instrumental era, but similar drought patterns can be found during the Medieval Climate Anomaly (MCA) (4). Typical North American droughts during the MCA were longer lasting (on the order of decades) and more intense (21), and were accompanied by large-scale dune mobilization over parts of the Great Plains (22). This movement of dunes implies a near-complete loss of vegetation cover (in this case induced naturally by an intense and persistent drought) and the possibility of a productive dust source and subsequent aerosol and vegetation feedbacks. Additionally, we note there are several areas in the world today where human land degradation (manifesting as loss of vegetation cover and increased vulnerability to wind erosion) and drought, potentially worsened by the subtropical drying that is projected to occur as a consequence of global warming (23, 24), have the potential to interact, leading to future Dust Bowl droughts in some developing regions (14). Both issues will require an integrated modeling approach, similar to the current study.

Model Description

All modeling experiments were conducted with the Goddard Institute for Space Studies (GISS) ModelE at 2° latitude by 2.5° longitude horizontal resolution and with 40 vertical layers (25). ModelE is a state-of-the-art atmospheric general circulation model, incorporating significant updates to the physics compared with previous versions and capable of calculating the evolution of several aerosol and chemical tracers as a function of the model climate (25, 26). Simulations of modern day climate in ModelE compare favorably with observations, with some notable biases, particularly in the subtropical marine stratocumulus regions. ModelE is unusually successful at simulating the observed annual cycle of precipitation over the Great Plains and Mexico, along with interannual variations in precipitation during the second half of the 20th century (27). We use a version of ModelE coupled to a model of soil dust aerosols (28). Given natural dust sources [i.e., excluding sources created by anthropogenic land degradation (29)] and forced by present-day ModelE climate, the dust model reproduces the seasonal atmospheric dust cycle as well as the magnitude and pattern of atmospheric dust loading (28, 30). Dust within the model interacts with

Table 1. Area averaged surface fluxes and TOA radiation balance for each ensemble simulation and difference from SST-ONLY for June–August period

Simulation	LH, Mean	SH, mean	LH+SH, mean	Bowen ratio	Net radiation, TOA
SST-ONLY	107.34	55.47	162.81	0.517	72.84
SST+CROP	101.72	59.62	161.34	0.586	73.17
SST+DUST	98.79	50.04	148.83	0.507	67.72
SST+DUST+CROP	94.40	51.62	146.03	0.547	67.77
Differences relative to SST-ONLY					
SST+CROP	−5.63	4.15	−1.48	0.069	0.334
SST+DUST	−8.56	−5.42	−13.98	−0.010	−5.122
SST+DUST+CROP	−12.94	−3.85	−16.79	0.030	−5.066

radiation in ModelE (absorbing, emitting, and reflecting longwave and shortwave) but does not impact cloud microphysics.

ACKNOWLEDGMENTS. We thank two anonymous reviewers for their comments. This work was supported by the National Oceanic and Atmospheric Administration (NOAA) Climate and Global Change Postdoctoral Fellowship Program, administered by the University Corporation for Atmospheric Research (B.I.C.), along with the Climate Dynamics Program of the National Science Foundation (NSF) through Grant ATM-06-20066. R.S. was supported by NOAA Grants NA03OAR4320179 and NA06OAR4310151 and NSF Grant ATM-05-01878. R.L.M. was additionally supported by the National Aeronautics and Space Administration Atmospheric Composition Program. This is Lamont contribution #7242.

1. Schubert SD, Suarez MJ, Pegion PJ, Koster RD, Bacmeister JT (2004) On the cause of the 1930s Dust Bowl. *Science* 303:1855–1859.
2. Schubert SD, Suarez MJ, Pegion PJ, Koster RD, Bacmeister JT (2004) Causes of long-term drought in the US Great Plains. *J Clim* 17:485–503.
3. Seager R, Kushnir Y, Herweijer C, Naik N, Velez J (2005) Modeling of tropical forcing of persistent droughts and pluvials over Western North America: 1856–2000. *J Clim* 18:4065–4088.
4. Seager R, et al. (2008) Would advance knowledge of 1930s SSTs have allowed prediction of the Dust Bowl drought? *J Clim* 21:3261–3281.
5. Cook BI, Miller RL, Seager R (2008) Dust and sea surface temperature forcing of the 1930s ''Dust Bowl'' drought. *Geophys Res Lett* 10.1029/2008GL033486.
6. Seager R, et al. (2005) Mechanisms of ENSO-forcing of hemispherically symmetric precipitation variability. *Q J R Meteorol Soc* 131:1501–1527.
7. McCabe GJ, Palecki MA, Betancourt JL (2004) Pacific and Atlantic Ocean influences on multidecadal drought frequency in the United States. *Proc Natl Acad Sci USA* 101:4136–4141.
8. Hoerling MP, Kumar A (2003) The perfect ocean for drought. *Science* 299:691–694.
9. Seager R (2007) The turn of the century North American drought: Global context, dynamics, and past analogs. *J Clim* 20:5527–5552.
10. Hansen ZK, Libecap GD (2004) Small farms, externalities, and the Dust Bowl of the 1930s. *J Polit Econ* 112:665–694.
11. Mitchell TD, Jones PD (2005) An improved method of constructing a database of monthly climate observations and associated high-resolution grids. *Int J Clim* 25:693–712.
12. Mattice WA (1935) Dust storms, November 1933 to May 1934. *Mon Weather Rev* 63:53–55.
13. Mattice WA (1935) Dust storms. *Mon Weather Rev* 63: 113–115.
14. Chepil WS (1957) Dust Bowl: Causes and effects. *J Soil Water Cons* 12:108–111.
15. Worster D (1979) *Dust Bowl: The Southern Plains in the 1930s* (Oxford Univ Press, New York).
16. Miller RL, Tegen I (1998) Climate response to soil dust aerosols. *J Clim* 11:3247–3267.
17. Yoshioka M, et al. (2007) Impact of desert dust radiative forcing on Sahel precipitation: Relative importance of dust compared to sea surface temperature variations, vegetation changes, and greenhouse gas warming. J Clim 20:1445–1467.
18. Zeng N, Neelin JD, Lau M-L, Tucker CJ (1999) Enhancement of interdecadal climate variability in the Sahel by vegetation interaction. *Science* 286:1537–1540.
19. Koven CD (2006) On the sources, composition, and climatic effects of mineral dust in the atmosphere. PhD Dissertation (Univ of California, Berkeley, CA).
20. Fye FK, Stahle DW, Cook ER (2003) Paleoclimate analogs to Twentieth-Century moisture regimes across the United States. *Bull Am Meteorol Soc* 84:901–909.
21. Herweijer C, Seager R, Cook ER, Emile-Geay J (2007) North American droughts of the last millennium from a gridded network of tree-ring data. *J Clim* 20:1353–1376.
22. Forman SL, Oglesby R, Webb RS (2001) Temporal and spatial patterns of Holcene dune activity on the Great Plains of North America: Megadroughts and climate links. *Glob Plan Change* 29:1–29.
23. Held IM, Soden BJ (2005) Robust responses of the hydrological cycle to global warming. *J Clim* 19:5686–5699.
24. Seager R, et al. (2007) Model projections of an imminent transition to a more arid climate in southwestern North America. *Science* 316:1181–1184.
25. Schmidt GA, et al. (2006) Present-day atmospheric simulation using GISS ModelE: Comparison to in situ, satellite, and reanalysis data. *J Clim* 19:153–192.
26. Shindell DT, et al. (2007) Climate response to projected changes in short-lived species under the A1B scenario from 2000–2050 in the GISS climate model. *J Geophys Res* 112 10.1029/2007JD008753.
27. Ruiz-Barradas A, Nigam S (2006) IPCC's twentieth-century climate simulations: Varied representations of North American hydroclimate. *J Clim* 19:4041–4058.
28. Miller RL, et al. (2006) Mineral dust aerosols in the NASA Goddard Institute for Space Sciences ModelE atmospheric general circulation model. *J Geophys Res* 111 10.1029/2005JD005796.
29. Ginoux P, et al. (2001) Sources and distributions of dust aerosols simulated with the GOCART model. *J Geophys Res* 106:20255–20274.
30. Cakmur RV, et al. (2006) Constraining the magnitude of the global dust cycle by minimizing the difference between a model and observations. *J Geophys Res* 111 10.1029/2005JD005791.